Bidirectional Transepithelial Water Transport: Measurement and Governing Mechanisms

Jonathan E. Phillips,*#§ Lid B. Wong,* and Donovan B. Yeates*§

Departments of *Medicine and #Chemical Engineering, University of Illinois at Chicago 60612, and §Department of Veterans Affairs, V.A. Chicago Health Care System, Chicago, Illinois 60612

ABSTRACT In the search for the mechanisms whereby water is transported across biological membranes, we hypothesized that in the airways, the hydration of the periciliary fluid layer is regulated by luminal-to-basolateral water transport coupled to active transepithelial sodium transport. The luminal-to-basolateral ($J_W^{L\rightarrow B}$) and the basolateral-to-luminal ($J_W^{B\rightarrow L}$) transepithelial water fluxes across ovine tracheal epithelia were measured simultaneously. The $J_W^{L\rightarrow B}$ (6.1 μl/min/cm^2) was larger than $J_W^{B\rightarrow L}$ (4.5 μl/min/cm^2, $p < 0.05$, $n = 30$). The corresponding water diffusional permeabilities were $P_d^{L\rightarrow B} = 1.0 \times 10^{-4}$ cm/s and $P_d^{B\rightarrow L} = 7.5 \times 10^{-5}$ cm/s. The activation energy (E_a) of $J_W^{L\rightarrow B}$ (11.6 kcal/mol) was larger than the E_a of $J_W^{B\rightarrow L}$ (6.5 kcal/mol, $p < 0.05$, $n = 5$). Acetylstrophanthidin (100 μM basolateral) reduced $J_W^{L\rightarrow B}$ from 6.1 to 4.4 μl/min/cm^2 ($p < 0.05$, $n = 5$) and abolished the PD. Amiloride (10 μM luminal) reduced $J_W^{L\rightarrow B}$ from 5.7 to 3.7 μl/min/cm^2 ($p < 0.05$, $n = 5$) and reduced PD by 44%. Neither of these agents significantly changed $J_W^{B\rightarrow L}$. These data indicate that in tracheal epithelia under homeostatic conditions, $J_W^{B\rightarrow L}$ was dominated by diffusion ($E_a = 4.6$ kcal/mol), whereas ~30% of $J_W^{L\rightarrow B}$ was coupled to the active Na^+,K^+-ATPase pump ($E_a = 27$ kcal/mol).

INTRODUCTION

The regulation of the transport of water across biological membranes is fundamental to life, the maintenance of homeostasis between body fluid compartments, and the preservation of the organism under adverse conditions. Specialized mechanisms in epithelia, endothelia, and other specialized membranes perform these regulatory functions. Osmosis, electroosmosis, pressure differentials, surface tension, and active ion-transport-coupled mechanisms have been proposed to control the net water flux across these membranes. These mechanisms work in concert, with the dominant mechanism being dependent on the membrane and its environmental conditions. Delineation of the relative importance of each of the potential mechanisms whereby water is transported across polarized biological membranes requires the manipulation of the potential mechanism(s) while making dynamic simultaneous measurements of transmembrane water transport in both directions.

The permeability of mammalian membranes and their facility in controlling water transport depend on their regulatory function. Epithelial membranes are commonly classified as "tight" or "leaky," which refer to their degree of paracellular junction tightness, which provides the main route for passive ion permeation (Fromter and Diamond, 1972). In leaky epithelia, which include small intestine, choroid plexus, gallbladder, and renal proximal tubule, the tight junctions have a high conductance, and the epithelial resistance is 4–300 Ω-cm^2 (Diamond, 1978). In tight epithelia, like the airway epithelia, frog skin, toad skin, and urinary bladder, the junctions have a low conductance and the resistance is >300 Ω-cm^2. It is usually assumed that tight membranes, with regard to ion transport, also have a low water P_d, with water transport and ion transport being interdependent. Leaky membranes are assumed to transport near-isotonic fluid, whereas in tight membranes, water transport has been proposed to be driven by either Na^+ and/or Cl^- transport. The discovery of water cotransport mechanisms (Zeuthen, 1996) reopens the possibility of membranes transporting hypotonic fluid, in other words, actively coupled transport of water.

The hydration of the airway lumen in the tracheobronchial epithelium is regulated such that the mucus atop the cilia is transported effectively by their rhythmic beating. In these converging branched airways, there is the potential for the depth of the periciliary and mucus layers of the mucociliary transport system to increase proximally. It has been proposed that the absorption of water by the airway epithelium keeps the mucus in close juxtaposition to the cilia (Wong and Yeates, 1997; Yeates et al., 1997), thus maintaining patent airways. In an airway lumen exposed to excess hydration, the transepithelial transport mechanism responsible for this mucosal-to-serosal transport of water is likely to be increased. It has been widely assumed, but not demonstrated in the tracheal epithelium, that this vectorial transport of water is linked to the luminal-to-basolateral transport of Na^+ (Matthay et al., 1996; Smith and Welsh, 1992). On the other hand, the basolateral-to-luminal transport of water has been proposed to be linked to the secretion of chloride into the airway lumen (Jiang et al., 1993; Oliver and Strang, 1974). The net transport of water, however, depends on the difference between these two vectorial water fluxes.

Received for publication 6 August 1998 and in final form 20 October 1998.

Address reprint requests to Dr. Donovan B. Yeates, Pulmonary Biophysics Laboratory, Department of Medicine, University of Illinois at Chicago (M/C 788), 1940 West Taylor Street, Chicago, IL 60612. Tel.: 312-996-6464; Fax: 312-996-1286; E-mail: yeates-d@uic.edu.

Dr. Wong's present address is LiDon Technologies LLC, Chicago, IL.

© 1999 by the Biophysical Society

0006-3495/99/02/869/09 $2.00

In the substantial series of investigations of ovine epithelia, Phipps and colleagues (Phipps et al., 1986, 1987, 1989) measured unidirectional water fluxes in adult epithelia of $J_W^{L\rightarrow B} = 3.4\ \mu l/min/cm^2$ and $J_W^{B\rightarrow L} = 3.3\ \mu l/min/cm^2$, using tritiated water (Phipps et al., 1989). These fluxes were large in comparison to the net flux. This is consistent with the small or negligible net water fluxes in native airway epithelia reported by other investigators (Duran et al., 1981; Folkesson et al., 1996; Loughlin et al., 1982; Welsh et al., 1980). Although open-circuit measurements of Na^+ and Cl^- transport in ovine tracheal epithelia have shown a net absorption of Na^+ and Cl^- (Cotton et al., 1983; Phipps et al., 1989), the mechanisms of the intracellular transport of either of these ions with vectorial water transport, in the absence of a secretagogue, have not been reported.

Herein we describe the fluorescent and electrophysiological techniques by which the mechanisms of water and ion transport were investigated in the ovine tracheal epithelium. To determine $J_W^{L\rightarrow B}$ and $J_W^{B\rightarrow L}$ across the same membrane simultaneously, a fluorescence system was developed that utilizes the higher quantum yield of 8-aminonapthalene-1,3,6-trisulfonic acid (ANTS) dissolved in D_2O compared to ANTS dissolved in H_2O. The vectorial water fluxes were derived from the temporal gradients of the number of fluorescent photons emitted by 1 mM ANTS present in the luminal and basolateral Hanks' balanced salt solutions (HBSS), which were prepared in H_2O and D_2O, respectively. To assess whether energy-dependent (active) processes were involved, the Arrhenius activation energy values (E_a) associated with the vectorial water fluxes were determined by measuring the water fluxes at 10, 20, 30, and 37°C. Unidirectional water fluxes and potential difference (PD, an indicator of active ion transport) were measured across native ovine tracheal epithelia in the absence and presence of inhibitors of the apical Na^+ channel and basolateral Na^+,K^+-ATPase. We show that under basal conditions, up to 30% of $J_W^{L\rightarrow B}$ was inhibited by inhibiting sodium absorption, whereas $J_W^{B\rightarrow L}$ was unaffected by Na^+ ion transport inhibitors. This, combined with the activation energy measurements, indicates that $J_W^{L\rightarrow B}$ was coupled to active ion transport and $J_W^{B\rightarrow L}$ was predominantly due to diffusion. These data predict that the homeostatic regulation of water in the airways can best be achieved by the manipulation of the mucosal-to-serosal vectorial water transport.

METHODS

System for measuring vectorial water fluxes and electrophysiological parameters

The measurement of unidirectional water fluxes exploits the properties of ANTS (Molecular Probes, Eugene, OR), which has a threefold higher quantum yield in D_2O than in H_2O (Stryer, 1966). Thus, when 1 mM ANTS is incorporated into HBSS (Hanks and Wallace, 1949) prepared in H_2O and in D_2O (99.9 atom % D; Sigma, St. Louis, MO), and these solutions are placed on either side of a membrane, the fluorescent intensity of the side containing D_2O decreases, whereas the fluorescence on the H_2O side increases as H_2O/D_2O moves across the membrane.

The system for measuring vectorial water fluxes across biological membranes, together with the electrophysiological properties of these membranes, is shown in Fig. 1. The system is designed to facilitate 1) the circulation of oxygenated media past each side of the membrane while minimizing the volume of the circulating fluid and its evaporative loss, 2) the measurements of transepithelial potential difference and short circuit current, 3) the measurements of the fluorescence of ANTS in the medium on each side of the membrane, and 4) regulation of the temperature of the circulating media. The main body of the apparatus is designated here as the fluorescence measurement unit. A removable flux cell holds the biological membrane under investigation. The fluorescence measurement unit and the flux cell are both constructed of black polycarbonate. Black polycarbonate is selected because it is biologically inert and opaque and has good machining and insulating properties. These, together with the associated pumps, proportional-integral-derivative (PID) temperature controllers, and an excitation light source, are mounted on a 500-pound marble table.

The flux cell (modified from Ussing, 1949) consists of two 500-μl chambers separated by the test membrane. Each chamber has two ports for the placement of salt bridges (glass barrel filled with 3 M KCl, plugged with porous ceramic) containing Ag^+/AgCl electrodes (no. 3433; Navi-Cyte, Reno, NV). A voltmeter and ammeter with current/voltage (I/V) clamp capabilities (DVC1000; WPI, Sarasota, FL) was used to measure the membrane's PD and Isc, respectively. The I/V clamp was also used to supply a current to clamp the membrane at a desired PD. Each chamber has an inlet and outlet for the circulation of HBSS. The membrane is retained by four sharp stainless steel pins located around the circumference of the luminal chamber, which mate with corresponding holes in the basolateral chamber. The two chambers are aligned by four locating rods. A handle protruding from the basolateral chamber activates a spring-loaded locking mechanism that provides the tension to ensure a liquid-tight seal between the chambers. O-rings seated around the inlet and outlet ports ensure a liquid-tight connection between the ports in the flux cell and the corresponding ports in the fluorescence measurement unit.

The fluorescence measurement unit contains a pair of 6-ml circulation loops, which are designed to facilitate the delivery of O_2 and CO_2 to the media and the measurement of a fluorescence probe in the media at a site remote from the tissue.

The oxygenation and pH of the luminal and basolateral bathing solutions are maintained by a 25 cm^3/min flow of a mixture of 95% O_2/5% CO_2 gas through each of a pair of 15-cm-long thin-walled (305 μm) silicon tubes (STSH-T-012; Sani-Tech, Lafayette, NJ) located within the circulation loops. This silicon tubing is gas but not water permeable. The gas mixture flows out of a constrictive orifice that vents to the atmosphere. Each loop also contains a type J thermocouple. The two circulation loops in the fluorescence measurement unit are completed when the flux cell is positioned in its cavity within the fluorescence measurement unit.

The temperature regulation and the circulation of the medium on each side of the membrane are maintained by two gear pumps (MP30MAG187; SciLog, Madison, WI), each with a Peltier heater/cooler (DT12–8; Marlow Industries, Dallas, TX) and associated water cooled heat sink mounted on the pump head (Fig. 1). These pumps circulate the HBSS at a flow rate of 20 ml/min past the surfaces of the membrane. This flow was selected because we found that the baseline water transport across the membrane remained constant at flow rates of 20 ml/min and above. Accurate control of the temperature in the flux cell between 10°C and 37°C was achieved by using the thermoelectric coolers in conjunction with the type J thermocouples and their respective PID temperature controllers (CN8500; Omega, Stamford, CT).

Each circulation loop contains a fluorescent measurement cell consisting of a 4-cm length of Suprasil quartz tubing with an inner diameter of 3 mm and an outer diameter of 5 mm (33458; Heraeus Amersil, Buford, GA). The excitation light entering through one hole in the fluorescence measurement unit illuminates the quartz tube, while a photomultiplier tube (PMT) in another hole, at a right angles to the illuminating light (Fig. 1), detects the emitted fluorescent photons. The excitation optics are enclosed in an antireflective, light-tight enclosure made of opaque black acrylic and metal tubing painted with optical black (3M; St. Paul, MN). To obtain the

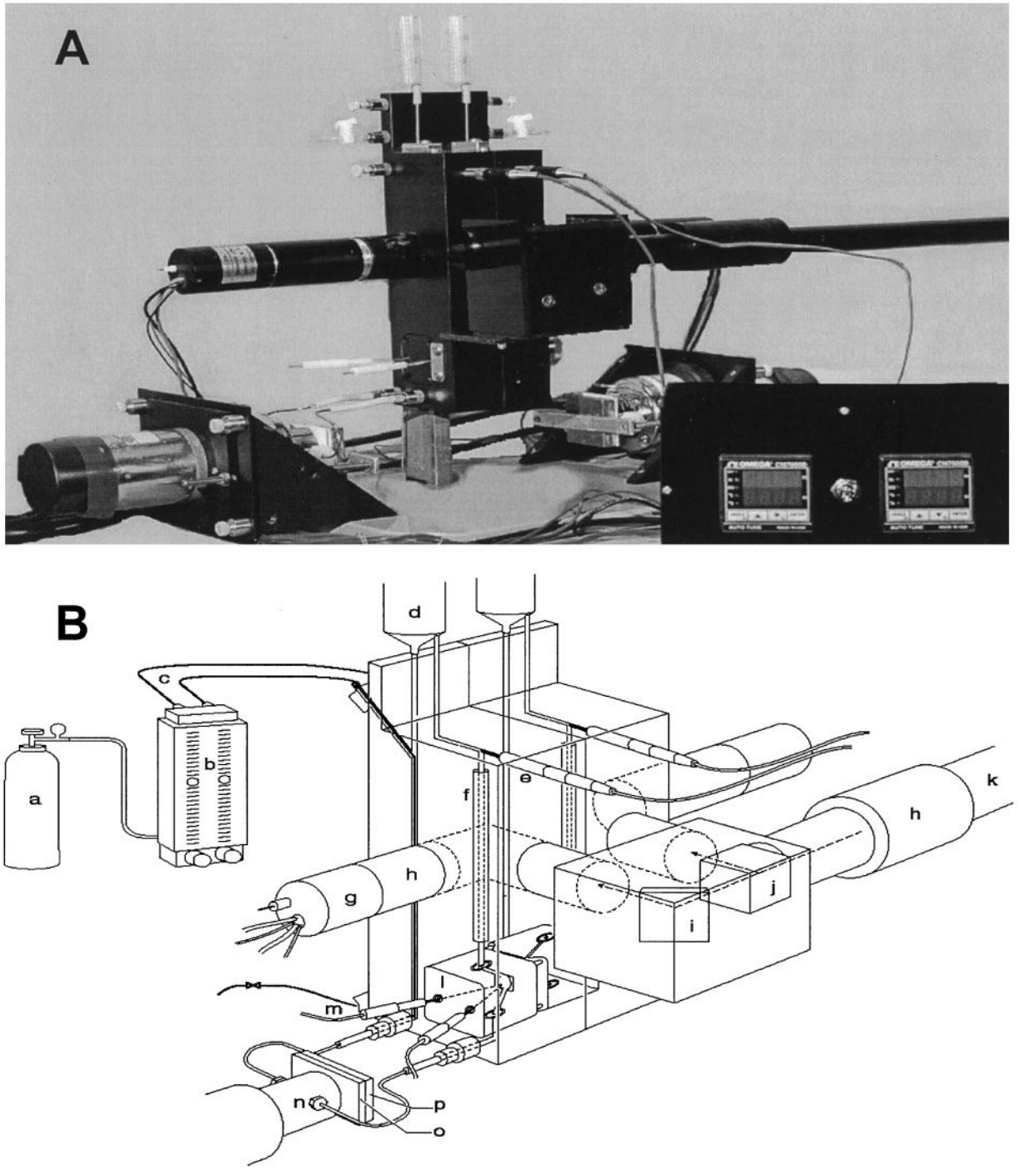

FIGURE 1 (*A*) Photograph of the water and ion transport measurement system for in vitro measurement of water flux and bioelectric parameters across biological membranes. (*B*) Schematic of the water and ion transport system. *a*, Compressed O_2/CO_2 tank; *b*, flowmeters; *c*, silicone tubing; *d*, balanced salt solution reservoirs; *e*, thermocouples; *f*, quartz tubing; *g*, photomultipler tubes; *h*, optical filters; *i*, mirror; *j*, beam splitter; *k*, from excitation light source (xenon lamp); *l*, removable flux cell; *m*, electrodes; *n*, gear pump; *o*, thermoelectric heater/cooler; *p*, water-cooled heat sink.

maximum fluorescent photon counts in the linear range of the PMTs, the excitation light from a 150-W xenon light source (L2175; Hamamatsu, Bridgewater, NJ) is first attenuated by a neutral density filter (0.86OD, Omega Optical, Brattleboro, VT). This excitation light is further filtered by a 380 ± 10-nm bandpass filter (03FIU014; Melles Griot, Irving, CA) and divided equally by a 25-mm cube beam-splitter (03BSC009; Melles Griot). One beam directly excites the D_2O/HBSS/ANTS flowing through the quartz tube in the basolateral chamber. The other beam is reflected by a 45° dichroic beamsplitter (66218; Oriel Corp., Stratford, CT). This beam excites the H_2O/HBSS/ANTS flowing through the quartz tube in the luminal chamber. The fluorescent photons from the D_2O/HBSS/ANTS and H_2O/HBSS/ANTS solutions pass through 515 ± 10 nm interference filters (C43,120; Edmund Scientific, Barrington, NJ) and are independently detected by their respective photon-counting PMTs (H3460-04; Hamamatsu). The amplifier/discriminator within the PMTs generates an emitter-coupled logic (ECL) pulse for each photon detected.

Data acquisition

The pulses from photomultiplier tubes are transmitted through 60-cm of 50-Ω cable to a custom-built circuit that generates one transistor-transistor logic (TTL) pulse for every two ECL pulses detected. The TTL pulses are counted in 1-s intervals by a counter board (DT2819; Data Translations, Marlboro, MA) interfaced to a personal computer. To convert the basolateral and luminal TTL pulse counts to photon counts per second (cps) and record them on the computer's hard disk, real-time data acquisition software (Real Time Toolbox; Humusoft, Praha, Czech Republic) written for the MatLab (The Mathworks, Natick, MA) platform is used. This software, in conjunction with an A/D board (PCL-711b; Advantech, Sunnyvale, CA), also records the PD or Isc, at 1 Hz, from the analog outputs on the *I*/*V* clamp.

Data reduction

The raw data were analyzed off-line and converted into unidirectional water flux values. Any outliers (spikes in the data) caused by environmental electromagnetic interference detected by the PMTs were removed with a running median filter (Evans, 1982). The background photon counts, measured before the start of each experiment with the system filled with pure H_2O/HBSS on both sides of the membrane, were stable. These counts were subtracted from the raw photon counts of each measurement. In a separate experiment it was found that the background photon counts did not change upon the addition of D_2O/HBSS to the system. The baseline of the fluorescence data was then suppressed by subtracting the fluorescent photon counts emitted by H_2O/HBSS/ANTS and normalized by the fluorescent photon counts emitted by D_2O/HBSS/ANTS. In the primarily H_2O chamber (luminal), the temporal increase in ANTS fluorescence caused by $J_W^{B\to L}$ (D_2O flux) entering the luminal chamber was used to calculate $J_W^{B\to L}$ (Fig. 2 *A*). In the primarily D_2O chamber (basolateral), the temporal decrease in ANTS fluorescence caused by $J_W^{L\to B}$ (H_2O flux) entering the basolateral chamber was used to calculate $J_W^{L\to B}$ (Fig. 2 *B*). The temporal change of the fluorescent photon counts in the basolateral and luminal solutions caused by the H_2O and D_2O fluxes across the membrane was derived from the slope of the linear regression performed every 10 s, using a 7-min window.

The diffusion permeability coefficient for water, P_d, expressed in cm/s, was calculated by the equation $P_d^{1\to 2} = J_w^{1\to 2}/\Delta C_w$, where $J_w^{1\to 2}$ is the vectorial water flux in mol/s/cm^2, and C_w is the concentration of H_2O (D_2O) on side one minus the concentration of H_2O (D_2O) on side two in (mol/cm^3).

Calibrations

The system was calibrated for transmembrane fluxes between 0 and 9.3 μl/min/cm^2. A water-impermeable Teflon (DuPont, Wilmington, DE) barrier was placed between the two chambers. The circulation loop in the fluorescence measurement unit irrigating the "luminal" side of the barrier was filled with 6 ml H_2O/HBSS/ANTS. The circulation loop in the fluorescence measurement unit irrigating the "basolateral" side of barrier was filled with 6 ml D_2O/HBSS/ANTS. The solutions were maintained at 37°C. Two syringe pumps (AS40A; Baxter, Round Lake, IL), one loaded with H_2O/HBSS/ANTS and infused into the basolateral circulation loop and one loaded with D_2O/HBSS/ANTS and infused into the luminal circulation loop, were set at flow rates of 0, 2, 5, 10, and 15 μl/min. The fluorescence calibration data are shown in Fig. 3. The change in fluorescence with respect to time for a constant flow rate was found to be linear over intervals of up to 2 h at these low flow rates. The background photon count was subtracted, the baseline was suppressed, and the resulting fluorescence data were normalized. The slope of these normalized data over time ($(dF/dt)_n$) was determined by linear regression for each corresponding calibration flux. To derive the temporal change (slope) of the fluorescent photon counts in the basolateral and luminal solutions, linear regression was performed every 10 s, using a 7-min window. Six flux measurements per minute were computed for each side of the membrane for 23 min. These flow rates were converted to a flux by dividing them by the area of the membrane (1.6 cm^2). These values comprise the analyzed calibration data (Fig. 4). Equations 1 and 2 within Fig. 4 are the linear regression fits of the analyzed calibration data. ANOVA for model selection proved that the linear models were statistically correct (no significant terms left out) for the calibration curves. These models make it possible to calculate $J_W^{L\to B}$ and $J_W^{B\to L}$ from the experimental fluorescence data.

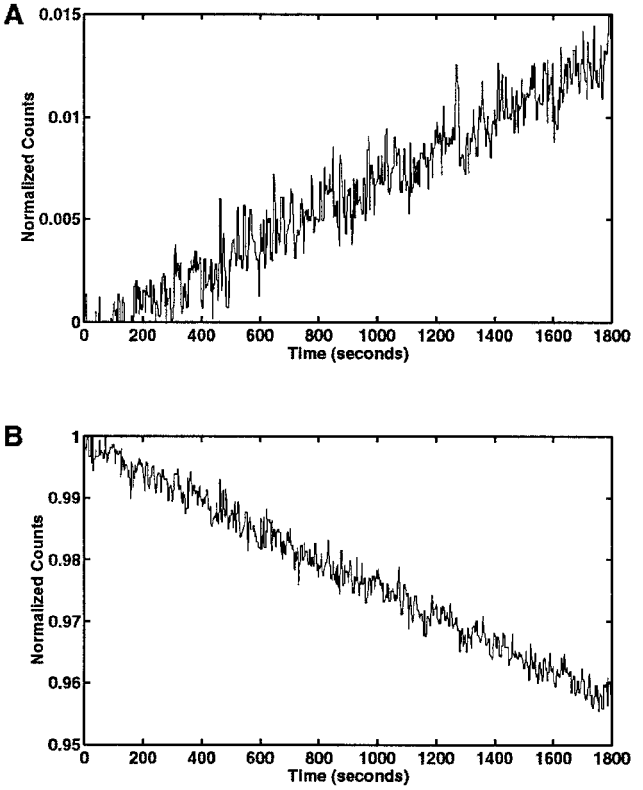

FIGURE 2 The figures show the background-subtracted, baseline-suppressed, normalized fluorescent photon counts. The increase in fluorescence (*A*) is used to calculate $J_w^{B\to L}$, and the decrease in fluorescence (*B*) is used to calculate $J_w^{L\to B}$.

Calibrations conducted at 10°C (lowest temperature used in this study) and 37°C (highest temperature) revealed that the $(dF/dt)_n$ for a given flow rate was unchanged over this temperature range, although the magnitude of the fluorescence of the ANTS was higher at 10°C than at 37°C. The zero flow rate calibration data showed that there was an apparent $J_W^{B\to L}$ of 0.07 ± 0.04 μl/min/cm^2 and an apparent $J_W^{L\to B}$ of 0.17 ± 0.12 μl/min/cm^2. These were not significantly different from zero flux.

Experimental procedure

Five sets of experiments were performed. Before each experiment the fluorescence measurement unit and flux cell were assembled without a membrane present. The system was filled with HBSS and allowed to equilibrate at 37°C. Any potential difference between the voltage-sensing electrodes was nulled, and the series resistance compensation circuitry was adjusted to compensate for the fluid resistance. The system was drained, and the flux cell removed.

Ovine tracheae, obtained at the local abattoir, were placed in HBSS at 4°C before transit to the laboratory. Each tracheum was cut longitudinally through the anterior aspect, exposing the posterior epithelium. Sheets of posterior epithelium were dissected free from the underlying connective tissue, smooth muscle, and cartilage. Tissues $\sim 1.3 \times \sim 1.3$ cm were mounted flat in the flux cell. The flux cell was inserted into the fluores-

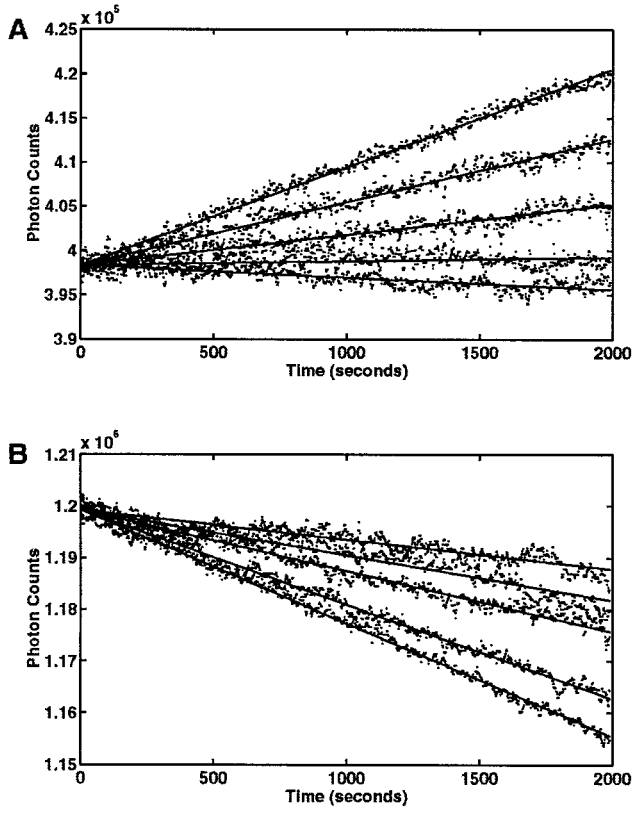

FIGURE 3 The luminal (*A*) and basolateral (*B*) raw 37°C calibration data. The increasing absolute slopes in each figure represent the 0, 1.24, 3.1, 6.2, and 9.3 μl/min/cm^2 calibration fluxes, respectively. The lines are the linear regression curve fits. In this figure the *y*-intercepts of the data were made to coincide.

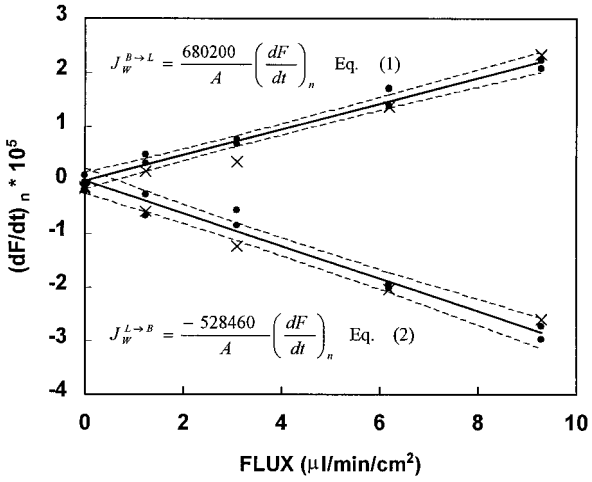

FIGURE 4 The water flux calibrations. The top line is represented by Eq. 1 and is the linear regression model for the $J_w^{B\to L}$ calibration data. The bottom line is represented by Eq. 2 and is the linear regression model for the $J_w^{L\to B}$ calibration data. The circles represent the 37°C calibration data, and the crosses are the 10°C calibration data. The dashed lines are the 95% confidence intervals on the linear models. The calibration curves have been corrected for photobleaching.

cence measurement unit. Both sides of the system were filled with H_2O/HBSS. 95% O_2/5% CO_2 was passed through the gas-permeable tubing, and the circulating medium was warmed to 37°C. Under these conditions the membrane PD stabilized in ~1 h. At this time both compartments were drained. The luminal side was flushed with 6 ml H_2O/HBSS/ANTS, and the basolateral side was flushed with 6 ml D_2O/HBSS/ANTS. Each side was refilled with its respective solution. The electrophysiological parameters were allowed to restabilize for ~30 min. The measurement of the fluorescence of the luminal and basolateral media was initiated after the electrophysiological values reached a steady state. At the commencement of each experiment, the baseline water flux and electrophysiological parameters of the membrane within the system were determined. The membrane's resistance (R_m) was calculated by dividing the open-circuit PD by the Isc.

The fluorescent photon counts from the luminal and basolateral bathing solutions were recorded for 30 min under open circuit conditions. The temporal changes in the fluorescent photon counts per second were used to calculate the basal $J_W^{L\to B}$ and $J_W^{B\to L}$. A $(dF/dt)_n$ value was calculated every 10 s, using the previous 7 min of fluorescent photon counts data. This was converted into a flux value by using the calibration curves. The average flux over a 30-min measurement period (138 flux values) was reported as the basal flux. The Isc was recorded at the beginning and end of the 30-min fluorescent data collection intervals.

Epithelia from 30 tracheae were studied in these experiments. The following five sets of experiments were conducted. Five tissues were used in four experiments and 10 in the other. In each of these tissues, the baseline water fluxes, PD, and Isc were measured before the commencement of the following experiments: 1) To determine if electroosmotic water transport could be detected, the responses of $J_W^{L\to B}$ and $J_W^{B\to L}$ were measured after the membrane potential difference was clamped at −50, −25, 0, open circuit, 25, and 50 mV. 2) To determine the unidirectional water flux activation energies, the unidirectional water fluxes were measured at 37, 30, 20, and 10°C. The activation energies (E_a) of the vectorial water fluxes were calculated from the slopes of the Arrhenius plots as $E_a = -\text{slope} \times R$, where R (1.987 cal/mol/K) is the ideal gas constant. 3) To determine if the luminal-to-basolateral water transport was coupled to the function of the basolateral Na^+,K^+-ATPase, the responses of $J_W^{L\to B}$, $J_W^{B\to L}$, and PD were measured after the addition of 100 μM acetylstrophanthidin (a Na^+,K^+-ATPase blocker) to the basolateral bathing solution. 4) To determine if the luminal-to-basolateral water transport was dependent on transcellular Na^+ transport, the responses of $J_W^{L\to B}$, $J_W^{B\to L}$, and PD were measured after the addition of 10 μM amiloride (a Na^+ channel blocker) to the luminal bathing solution. 5) The baseline water fluxes, PD, and Isc were measured for an additional 10 tissues, each from a separate trachea.

Data analysis

The $J_W^{L\to B}$, $J_W^{B\to L}$, PD, Isc, and R_m from the studies were summarized as means ± SE. Paired difference, two-tailed, Student's *t*-tests were performed to determine whether the differences/changes in vectorial water flux, activation energy, and electrophysiological values were significant at a *p*-value less than or equal to 0.05. Statistical significance of the difference between the calculated net flux and zero at a *p*-value less than 0.05 was evaluated by a two-tailed, Student's *t*-test using the error propagated from the vectorial fluxes.

RESULTS

The electrophysiological properties of the 30 ovine tracheal tissues demonstrated that the viability of tissues was maintained for over 6 h. These 30 tissues had a mean basal PD of 11.7 ± 1.1 mV (lumen negative) and generated a short circuit current of 37 ± 4 μA/cm^2. This resulted in a mean tissue resistance of 362 ± 33 Ω-cm^2. The airway epithelia were absorptive, with the $J_W^{L\to B}$ of 6.1 ± 0.3 μl/min/cm^2 greater than the $J_W^{B\to L}$ of 4.5 ± 0.3 μl/min/cm^2 ($p < 0.05$,

$n = 30$), and this net flux of 1.6 μl/min/cm^2 was significantly different from zero ($p < 0.05$, $n = 30$).

The I/V curves were curvilinear. A characteristic curve generated by clamping the PD of the tissue between -50 and 50 mV is shown in Fig. 5. The slope, which is representative of the R_m, was essentially linear within the physiological range. There was little change in the corresponding vectorial water fluxes over the PD range of -25 to 50 mV, whereas when the membrane was clamped at -50 mV there was a 70% increase in $J_W^{B\to L}$ over the open circuit $J_W^{B\to L}$ (data not shown). The mean $J_W^{L\to B}$ followed a trend in which it increased as the clamped potential was changed from 50 to -50 mV. Thus we were unable to demonstrate any electroosmotically driven water transport over this range. The 70% increase in $J_W^{B\to L}$ at high lumen negative PD could be interpreted as electroosmotic water transport associated with paracellular Cl^- absorption.

The logarithmic decreases in $J_W^{L\to B}$ and $J_W^{B\to L}$ versus the increases in the reciprocal of the absolute temperature of the circulating media are shown in Fig. 6. The linearity of the plots was taken to indicate that vectorial water flux obeyed a simple Arrhenius equation ($J_w = A \exp(-E_a/RT)$), where A is a constant. The average E_a for $J_W^{L\to B}$ of 11.6 $\pm$ 1.2 kcal/mol was greater than the E_a for $J_W^{B\to L}$ of 6.5 $\pm$ 0.7 kcal/mol ($p < 0.05$, $n = 5$).

Acetylstrophanthidin caused a slow decrease (τ = 1710 $\pm$ 131 s) in the absolute PD toward zero mV (Fig. 7), where τ is the time in seconds required for the PD to decrease to 63.3% of its total change. This specific Na^+,K^+-ATPase inhibitor decreased $J_W^{L\to B}$ from 6.1 $\pm$ 0.5 to 4.4 $\pm$ 0.7 μl/min/cm^2 ($p < 0.05$), whereas the decrease in $J_W^{B\to L}$ from 4.8 $\pm$ 0.3 to 4.6 $\pm$ 0.3 μl/min/cm^2 did not reach statistical significance ($p = 0.07$). The net flux (J_W^{NET}), calculated by subtracting $J_W^{L\to B}$ from $J_W^{B\to L}$, was 1.3 $\pm$ 0.6 μl/min/cm^2 before the addition of acetylstrophanthidin and -0.2 $\pm$ 0.7 μl/min/cm^2 after, perhaps revealing a trend ($p = 0.18$) in which the normally absorptive membrane secreted upon the addition of acetylstrophanthidin.

Amiloride caused a rapid (τ = 31 $\pm$ 9 s) decrease in the absolute PD (Fig. 8) to 44% of the baseline value. The membrane resistance was 430 $\pm$ 80 Ω-cm^2 compared to 410 $\pm$ 78 Ω-cm^2 ($p = 0.30$) after the addition of amiloride.

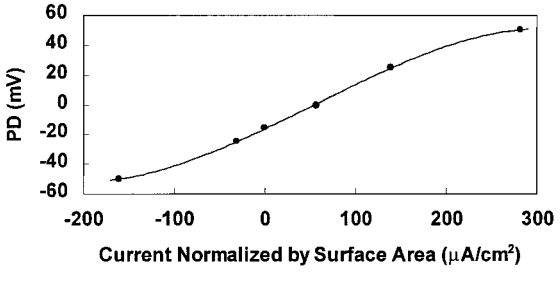

FIGURE 5 The current/voltage relationship for an ovine tracheal epithelium. The current normalized by surface area required to maintain a selected PD was recorded. A membrane resistance normalized by a surface area of 281 Ω-cm^2 was determined for this membrane.

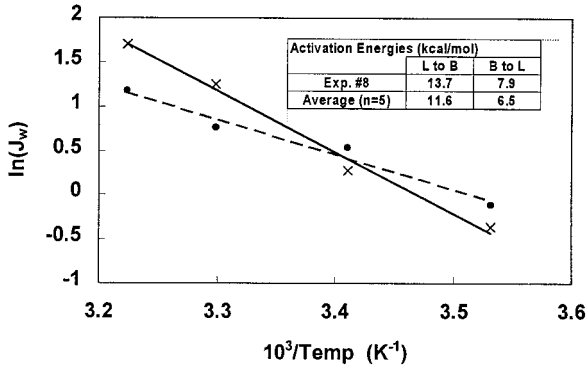

FIGURE 6 Arrhenius plots of the temperature dependence of $J_w^{L\to B}$ (——) and $J_w^{B\to L}$ (– – –). The circles represent individual determinations of $J_w^{B\to L}$ from experiment 8 and are fitted with the line $y = -4.0x + 13.9$. The crosses represent individual determinations of $J_w^{L\to B}$ from experiment 8 and are fitted with the line $y = -6.9x + 24.1$. The E_a that was calculated for experiment 8 and the average E_a ($n = 5$) are summarized in the inset.

Amiloride caused a decrease in $J_W^{L\to B}$ from 5.7 $\pm$ 0.6 to 3.7 $\pm$ 0.5 μl/min/cm^2 ($p < 0.05$). $J_W^{B\to L}$ was 4.0 $\pm$ 0.6 μl/min/cm^2 before amiloride and 3.9 $\pm$ 0.5 μl/min/cm^2 after the addition of amiloride ($p = 0.77$). J_W^{NET} was 1.7 $\pm$ 0.9 μl/min/cm^2 before the addition of amiloride and -0.3 $\pm$ 0.7 μl/min/cm^2 after amiloride, revealing a trend ($p = 0.14$) in which the normally net water absorptive membrane secreted water upon the addition of amiloride.

If the baseline vectorial water fluxes are assumed to be purely diffusive, then the calculated diffusional permeability coefficient values are $P_d^{L\to B} = 10 \pm 0.6 \times 10^{-5}$ cm/s and $P_d^{B\to L} = 7.5 \pm 0.5 \times 10^{-5}$ cm/s. However, as we have shown herein that $J_W^{L\to B}$ (and perhaps $J_W^{B\to L}$) was coupled to an active process(es), the water fluxes cannot be assumed to be purely Fickian. On the assumption that acetylstrophanthidin suppresses all active water transport, the calculated P_d value(s) are $P_d^{L\to B}$ of 7.4 $\pm$ 1.1 $\times$ 10^{-5} cm/s and $P_d^{B\to L}$ of 7.6 $\pm$ 0.5 $\times$ 10^{-5} cm/s.

DISCUSSION

Herein we have demonstrated the utilization of a novel system for measuring bidirectional transmembrane water

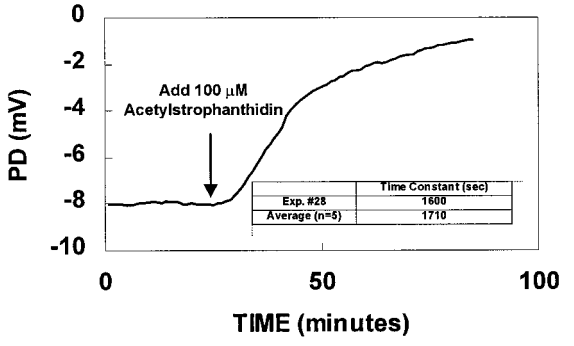

FIGURE 7 The decrease in the absolute magnitude of the PD of an ovine tracheal epithelium induced by acetylstrophanthidin on PD. The time constants for acetylstrophanthidin are summarized in the inset.

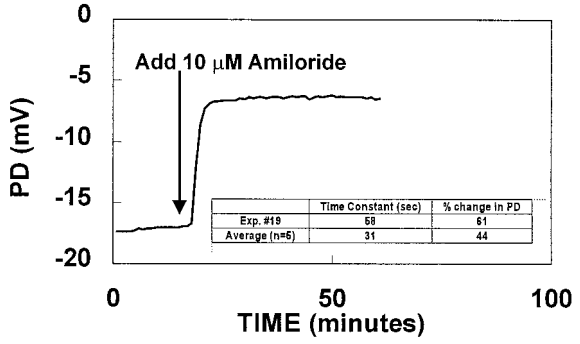

FIGURE 8 An example of the rapid decrease in the absolute magnitude of the PD of an ovine tracheal epithelium induced by amiloride. The amiloride time constants and increases in PD are summarized in the inset.

transport. The unidirectional water fluxes across native tracheal epithelium in either direction were relatively large ($\sim$5 μl/min/cm^2), which is consistent with an epithelium of intermediate ion permeability. The difference between the luminal-to-basolateral and the basolateral-to-luminal water transports resulted in an average net absorption of 1.6 μl/min/cm^2, only a fraction of the unidirectional fluxes. The activation energy of the luminal-to-basolateral water flux (11.6 kcal/mol) was considerably higher than the activation energy of the self-diffusion of water (4.6 kcal/mol; Wang et al., 1953), providing evidence that this water transport was coupled to or associated with an active cellular process(es). That the activation energy of the basolateral-to-luminal water flux (6.5 kcal/mol) was considerably lower than that of the luminal-to-basolateral water flux but slightly higher than 4.6 kcal/mol suggests that in the nonchallenged state, the basolateral-to-luminal water transport is governed largely by diffusional processes (likely through aquaporins and/or the paracellular spaces), with the possibility that an actively coupled component is present. The 30% decrease in the luminal-to-basolateral water transport caused by inhibition of the basolateral Na^+,K^+-ATPase with acetylstrophanthidin is consistent with the concept that transcellular transport of water is coupled with either Na^+ transport or at least the operation of the Na^+,K^+-ATPase pump. The decrease in this water transport by inhibition of the apical sodium channel with amiloride indicates that this transepithelial water transport was associated with the transcellular transport of Na^+. This is the first quantitative demonstration that in the nonchallenged state, transepithelial water transport from the tracheal airway lumen to the submucosa is coupled to and/or regulated by transcellular active sodium transport, whereas the basolateral-to-luminal transport of water appears to be predominantly diffusive.

The magnitudes of the open-circuit unidirectional transepithelial water transport measurements reported herein in native sheep tracheal mucosa are similar to the magnitudes of $J_W^{L\rightarrow B}$ (3.4 μl/min/cm^2), $J_W^{B\rightarrow L}$ (3.2 μl/min/cm^2), $P_d^{L\rightarrow B}$ (5.1×10^{-5} cm/s), and $P_d^{B\rightarrow L}$ (4.6×10^{-5} cm/s) measured by Phipps and colleagues (Phipps et al., 1989). It is possible that our values are slightly higher than those reported by Phipps, as our small chamber volume and rapid circulation likely resulted in smaller boundary layers than the 550 μm estimated in their bubble-lift system. As those investigators measured the unidirectional fluxes by using tritiated water, it was not possible for their measurements of $J_W^{L\rightarrow B}$ and $J_W^{B\rightarrow L}$ to be made simultaneously, as ours were. Thus, it is not surprising that their $J_W^{L\rightarrow B}$ was not statistically larger that their $J_W^{B\rightarrow L}$.

Considering the difference in size between the sheep and a ferret, it is not surprising that a water absorption rate of 0.5 μl/min/trachea (Loughlin et al., 1982) was reported. Other investigators have reported minimal, if any, water transport in native epithelium under resting conditions (Duran et al., 1981; Phipps et al., 1989; Welsh et al., 1980). Measurements of net water transport in cultured cells have mostly been reported to be absorptive, but only 1/50 (0.03 μl/min/cm^2; Jiang et al., 1993) of the net water flux reported herein for native epithelia. Such measurements in cultured epithelia challenge the accuracy of the volumetric methodologies used. Moreover, epithelia in culture have higher resistance (1000 Ω-cm^2; Jiang et al., 1993) and lower aquaporin expression (Ruddy et al., 1998) and may have lost some of their intrinsic mechanisms that facilitate the regulation of water transport within and across the cells.

These are the first simultaneous measurements of the E_a of $J_W^{L\rightarrow B}$ and the E_a of $J_W^{B\rightarrow L}$ across biological membranes. Our $J_W^{L\rightarrow B}$ water flux activation energy of 11.6 kcal/mol is remarkably similar to that reported for toad bladder epithelia of 11.7 kcal/mol (Hays et al., 1971). This elegant work studied the influence of boundary layers as well as the supporting layer of cells under the epithelium on the measured E_a. Hays et al. determined that boundary layers and the supporting layer of cells under the epithelium were not of importance when the baseline E_a was measured but were important when the epithelium was made more permeable by vasopressin. This supports our implicit assumption that under baseline conditions the rate-limiting step for water transport lies within the epithelial cell layer. The large decrease in the luminal-to-basolateral water flux with decreasing temperature is indicative that water transport is not purely Fickian but is due to an active process. The E_a of water transport through a nonporous lipid bilayer has been reported to be 13 kcal/mol because of solubility and diffusion mechanisms in series (Price and Thompson, 1969). We believe that water transport through the lipid bilayer is unlikely to contribute substantially to our measured E_a of 11.6 kcal/mol, as the E_a of $J_W^{B\rightarrow L}$ is low and there is no a priori reason to suggest that a rectifying mechanism can be attributed to the intrinsic properties of the lipid membranes of the epithelial cells. It is likely that the higher E_a of $J_W^{L\rightarrow B}$ is coupled to the Na^+,K^+-ATPase located on the basolateral side of the epithelium. Na^+,K^+-ATPase has an E_a of 27 kcal/mol (Apell et al., 1985). The E_a for water diffusion through the paracellular spaces and aquaporins are similar and should be close to 4.6 kcal/mol (Finkelstein, 1987). Based on our data and these assumptions, we conclude that the $J_W^{L\rightarrow B}$ is in a large part due to diffusive processes, with

an actively coupled regulatory component. Thus, in polarized airway epithelia, the higher E_a for $J_W^{L\rightarrow B}$ than $J_W^{B\rightarrow L}$ under basal conditions is consistent with its regulatory function.

The unidirectional fluxes through the membranes used herein, of thickness ~1.5 mm, ranged between 2.1 and 8.6 μl/min/cm^2. According to Fick's First Law, the flux due to self-diffusion of water at 37°C through 1.5 mm is 11.6 μl/min/cm^2. Thus the epithelium retards the diffusion of water to roughly one-fourth to one-half that of free water, with the regulation of the net flux primarily controlled by the regulation of $J_W^{L\rightarrow B}$ in the basal state. It is reasonable to assume that the large unidirectional water fluxes (~2.8×10^{-4} mol H_2O/min/cm^2) are predominantly diffusive, with non-Fickian fluxes associated with active ion (Na^+ and Cl^-) transport.

The likely source of energy for this water transport is the basolateral Na^+,K^+-ATPase pump. Ovine tracheal epithelia, under open-circuit conditions, were shown to absorb both Na^+ and Cl^- (Phipps et al., 1989). We have shown that ~30%, or ~2 μl/min/cm^2, of the $J_W^{L\rightarrow B}$ was inhibited by agents that inhibit sodium transport, providing the evidence that $J_W^{L\rightarrow B}$ follows luminal-to-basolateral Na^+ transport in the basal state. It is noteworthy that similar decreases in $J_W^{L\rightarrow B}$ were observed with inhibition of the basolateral Na^+,K^+-ATPase and the apical sodium channels, which cause cell swelling and shrinkage, respectively.

The system was designed to be thermodynamically closed to water transport and to minimize the volume on each side of the tissue, and thus maximize the change in fluorescence due to the transmembrane transport of H_2O and D_2O. Our threefold increase in D_2O over H_2O HBSS is similar to the 3.2-fold increase in fluorescence in D_2O over H_2O found by Kuwahara and Verkman in their salt solutions (Kuwahara and Verkman, 1988) and consistent with the 3.7-fold increase in quantum yield in pure D_2O over pure H_2O solvents (Stryer, 1966). The resolution of the bidirectional water transport was limited by the upper counting limitations of the photomultiplier tubes and the rate of sampling of these counts. The error in the determination of the unidirectional flux measurements was propagated when the unidirectional fluxes were subtracted, yielding a small value for the net flux with comparatively large standard deviation. The diffusion of D_2O is only slightly lower than H_2O and thus is not a major source of error. Other investigators have found the isotopic effects of D_2O to be minimal (Hevesy et al., 1935; Kuwahara and Verkman, 1988; Lucke and Harvey, 1935), although this may not be universally true (Brink, 1983; Brooks, 1936; Lawaczeck, 1984). We conducted preliminary experiments with D_2O on the luminal side, where $J_W^{B\rightarrow L} = 5.2 \pm 1.0$ μl/min/cm^2 ($n = 5$). This value can be compared to these experiments with H_2O on the luminal side, where $J_W^{B\rightarrow L} = 5.0 \pm 1.3$ μl/min/cm^2 ($n = 5$) under the same conditions. Furthermore, the PD values before the addition of D_2O to the system (-12.4 ± 1.0 mV) were not significantly different from values recorded after the addition of D_2O to the basolateral side (-11.7 ± 1.1 mV, $p = 0.64$, $n = 30$). Thus, as far as can be ascertained, D_2O and H_2O are physiologically similar in the tissue in these experiments.

Acetylstrophanthidin caused a more rapid decrease in absolute PD than ouabain in an ovine tracheal tissue. Both cardiac glycosides decreased the PD toward zero. These data are comparable with the decreases and temporal changes in PD induced by ouabain in dog tracheal epithelia (Al-Bazzaz and Al-Awqati, 1979). The time course and effect on PD we observed for amiloride are consistent with what others have observed in sheep (Cotton et al., 1983) and canine (Al-Bazzaz and Al-Awqati, 1979) airway epithelia.

These investigations elucidate mechanisms whereby the predicted water absorption occurring as secretions are transported centripetally in the converging branched tracheobronchial tree. The data support those reported by Winters and Yeates (1997), who showed that acetylstrophanthidin increased bronchial mucociliary clearance in dogs. In concert, they indicate that under homeostasis, the regulation of the actively coupled luminal-to-basolateral flux of water may be more amenable to pharmacological manipulation in terms of both magnitude and mechanism than the predominantly diffusive basolateral-to-luminal water flux. We conclude that the inhibition of transepithelial Na^+ transport increases the periciliary fluid layer depth by decreasing $J_W^{L\rightarrow B}$. These data indicate that diseased airways with inspissated mucus may be rehydrated by pharmacological manipulation of transepithelial Na^+ and water transport to reestablish effective mucociliary function.

This work is based on a thesis of J. Phillips, to be submitted in partial fulfillment of the requirements for the Doctor of Philosophy degree from the department of Chemical Engineering, University of Illinois at Chicago. The authors are grateful to Dr. Irving F. Miller for his advice and guidance during the preparation of the manuscript. The authors thank Matt Schuck for constructing the water and ion transport measurement system and Bob Kulseth for designing the ECL-to-TTL flip-flop converter. A preliminary report of this work was given at the 1998 American Lung Association/American Thoracic Society International Conference and published in abstract form (*Am. J. Respir. Crit. Care Med.* 157:A848).

JEP was awarded the Sigma Xi Philip Hawley award for this work. JEP was also the recipient of an Amoco foundation doctoral fellowship, 1994–1996. This work was supported in part by a grant from the Medical Service of the Department of Veterans Affairs.

REFERENCES

Al-Bazzaz, F. J., and Q. Al-Awqati. 1979. Interaction between sodium and chloride transport in canine tracheal mucosa. *J. Appl. Physiol.* 46: 111–119.

Apell, H. J., M. M. Marcus, B. M. Anner, H. Oetliker, and P. Lauger. 1985. Optical study of active ion transport in lipid vesicles containing reconstituted Na,K-ATPase. *J. Membr. Biol.* 85:46–63.

Brink, P. R. 1983. Effect of deuterium oxide on junctional membrane channel permeability. *J. Membr. Biol.* 71:79–87.

Brooks, S. C. 1936. The permeability of erythrocytes to deuterium oxide. *J. Cell. Comp. Physiol.* 7:163–171.

Cotton, C. U., E. E. Lawson, R. C. Boucher, and J. T. Gatzy. 1983. Bioelectric properties and ion transport of airways excised from adult and fetal sheep. *J. Appl. Physiol.* 55:1542–1549.

Diamond, J. M. 1978. Channels in epithelial cell membranes and junctions. *Fed. Proc.* 37:2639–2644.

Duran, J., W. Duran, and P. Haab. 1981. Volume flow, hydraulic conductivity and electrical properties across bovine tracheal epithelium in vitro: effect of histamine. *Pflugers Arch.* 392:40–45.

Evans, J. R. 1982. Running median filters and a general despiker. *Bull. Seism. Soc. Am.* 72:331–338.

Finkelstein, A. 1987. Water Movement through Lipid Bilayers, Pores, and Plasma Membranes. John Wiley and Sons, New York.

Folkesson, H. G., M. A. Matthay, A. Frigeri, and A. S. Verkman. 1996. Transepithelial water permeability in microperfused distal airways. *J. Clin. Invest.* 97:664–671.

Fromter, E., and J. Diamond. 1972. Route of passive ion permeation in epithelia. *Nature New Biol.* 235:9–13.

Hanks, J. H., and R. E. Wallace. 1949. Relation of oxygen and temperature in the preservation of tissues by refrigeration. *Proc. Soc. Exp. Biol. Med.* 71:196–200.

Hays, R. M., N. Franki, and R. Soberman. 1971. Activation energy for water diffusion across the toad bladder. *J. Clin. Invest.* 50:1016–1018.

Hevesy, G. V., E. Hofer, and A. Krogh. 1935. The permeability of the skin of frogs to water as determined by D_2O and H_2O. *Skand. Arch. Physiol.* 72:199–214.

Jiang, C., W. E. Finkbeiner, J. H. Widdicombe, P. B. McCray, and S. S. Miller. 1993. Altered fluid transport across airway epithelium in cystic fibrosis. *Science.* 262:424–427.

Kuwahara, M., and A. S. Verkman. 1988. Direct fluorescence measurement of diffusional water permeability in the vasopressin-sensitive kidney collecting tubule. *Biophys. J.* 54:587–593.

Lawaczeck, R. 1984. Water permeability through biological membranes by isotopic effects of fluorescence and light scattering. *Biophys. J.* 45: 491–494.

Loughlin, M., G. A. Gerencser, M. A. Crowder, R. L. Boyd, and J. A. Mangos. 1982. Fluid fluxes in ferret trachea. *Experientia.* 38: 1451–1452.

Lucke, B., and E. N. Harvey. 1935. The permeability of living cells to heavy water. *J. Cell. Comp. Physiol.* 5:473–482.

Matthay, M. A., H. G. Folkesson, and A. S. Verkman. 1996. Salt and water transport across alveolar and distal airway epithelia in the adult lung. *Am. J. Physiol.* 270:L487–L503.

Oliver, R. E., and L. B. Strang. 1974. Ion fluxes across the pulmonary epithelium and the secretion of lung liquid in the foetal lamb. *J. Physiol. (Lond.).* 241:327–357.

Phipps, R. J., W. M. Abraham, A. T. Mariassy, P. J. Torrealba, M. W. Sielczac, A. Ahmed, M. McCray, J. S. Stevenson, and A. Wanner. 1989. Developmental changes in the tracheal mucociliary system in neonatal sheep. *J. Appl. Physiol.* 67:824–832.

Phipps, R. J., S. M. Denas, M. W. Sielczak, and A. Wanner. 1986. Effects of 0.5 ppm ozone on glycoprotein secretion, ion, and water fluxes in sheep trachea. *J. Appl. Physiol.* 60:918–927.

Phipps, R. J., P. J. Torrealba, I. T. Lauredo, S. M. Denas, M. W. Sielczak, A. Ahmed, W. M. Abraham, and A. Wanner. 1987. Bacterial peneumonia stimulates macromolecule secretion and ion and water fluxes in sheep trachea. *J. Appl. Physiol.* 62:2388–2397.

Price, H. D., and T. E. Thompson. 1969. Properties of liquid bilayer membranes separating two aqueous phases: temperature dependence of water permeability. *J. Mol. Biol.* 41:443–457.

Ruddy, M. K., J. M. Drazen, O. M. Pitkanen, B. Rafii, H. M. O'Brodovich, and H. W. Harris. 1998. Modulation of aquaporin 4 and the amiloride-inhibitable sodium channel in perinatal rat lung epithelial cells. *Am. J. Physiol.* 274:L1066–L1072.

Smith, J. J., and M. J. Welsh. 1992. cAMP stimulates bicarbonate secretion across normal, but not cystic fibrosis airway epithelia. *J. Clin. Invest.* 89:1148–1153.

Stryer, L. 1966. Excited-state proton-transfer reactions. A deuterium isotope effect on fluorescence. *J. Am. Chem. Soc.* 88:5708–5712.

Ussing, H. H. 1949. The active ion transport through the isolated frog skin in the light of tracer studies. *Acta Physiol. Scand.* 17:1–37.

Wang, J. H., C. V. Robinson, and I. S. Edelman. 1953. Self-diffusion and structure of liquid water. *J. Am. Chem. Soc.* 75:466–470.

Welsh, M. J., J. H. Widdicombe, and J. A. Nadel. 1980. Fluid transport across the canine trachela epithelium. *J. Appl. Physiol.* 49:905–909.

Winters, S. L., and D. B. Yeates. 1997. Roles of hydration, sodium, and chloride in regulation of canine mucociliary transport system. *J. Appl. Physiol.* 83:1360–1369.

Wong, L. B., and D. B. Yeates. 1997. Dynamics of the regulation of ciliated epithelial function. *Comments Theor. Biol.* 4:183–208.

Yeates, D. B., G. J. Besseris, and L. B. Wong. 1997. Physicochemical properties of mucus and its propulsion. *In* The Lung: Scientific Foundations. R. Crystal and J. West, editors. Raven, Philadelphia. 487–503.

Zeuthen, T. 1996. Molecular Mechanisms of Water Transport. R. G. Landes Co., Austin, TX.